HEAT TRANSFER AND FLOW REGION CHARACTERISTICS STUDY IN A NON-ANNULAR CHANNEL BETWEEN ROTOR AND STATOR

by

Mahdi NILI-AHMADABADI and Hadi KARRABI *

Faculty of Mechanical Engineering, Isfahan University of Technology, Isfahan, Iran

Original scientific paper
DOI: 102298/TSCI110702138M

This paper will present the results of the experimental investigation of heat transfer in a non-annular channel between rotor and stator similar to a real generator. Numerous experiments and numerical studies have examined flow and heat transfer characteristics of a fluid in an annulus with a rotating inner cylinder. In the current study, turbulent flow region, and heat transfer characteristics have been studied in the air gap between the rotor and stator of a generator. The test rig has been built in a way which shows a very good agreement with the geometry of a real generator. The boundary condition supplies a non-homogenous heat flux through the passing air channel. The experimental devices and data acquisition method are carefully described in the paper. Surface-mounted thermocouples are located on the both stator and rotor surfaces and one slip ring transfers the collected temperature from rotor to the instrument display. The rotational speed of rotor is fixed at three under: 300 rpm, 900 rpm, and 1500 rpm. Based on these speeds and hydraulic diameter of the air gap, the Reynolds number has been considered in the range: 4000 < Re_z < < 30000. Heat transfer and pressure drop coefficients are deduced from the obtained data based on a theoretical investigation and are expressed as a formula containing effective Reynolds number. To confirm the results, a comparison is presented with Gazley's data report. The presented method and established correlations can be applied to other electric machines having similar heat flow characteristics.

Key words: *heat transfer, turbulent flow, forced convection, effective Reynolds, number experimental study*

Introduction

Taylor [1] investigated stability of static fluid between two concentric cylinders with rotating inner cylinder. He observed Taylor's vortex in velocity values more than critical rotational velocity. Instability of laminar flow causes formation of this vortex. Increasing centrifugal force and radius cause this instability. Taylor number for formation of vortex in the annular flow with two enclosed ends corresponds with $Ta_{cr} > 41.2$ in which Taylor number is defined as following:

* Corresponding author; e-mail: h.karrabi@yahoo.com

$$\mathrm{Ta}_{\mathrm{cr}} = \frac{V(D_{\mathrm{o}} - D_{\mathrm{i}})}{2\upsilon}\sqrt{\frac{D_{\mathrm{h}}}{D_{\mathrm{m}}}} \tag{1}$$

The results of Taylor show that getting turbulent flow depends on the ratio of radius of inner cylinder to width of air gap. Critical rotational Reynolds number in which laminar flow changes to turbulence flow correspond:

$$\mathrm{Re}_{\mathrm{cr}} = 41.1\sqrt{\frac{D_{\mathrm{o}}}{D_{\mathrm{i}}} - 1} \tag{2}$$

Pia [2] experimented laminar and turbulent annular flow between two concentric cylinders. His results show that rotation of inner cylinder induces vortexes in both laminar and turbulent regions as in the laminar flow region; axis of vortex and axis of rotation are orthogonal whereas in the turbulent flow region, axis of vortex and axis of rotation are not orthogonal.

Chandrasekhar [3] reported that by adding axial flow to rotational flow, stability of annular flow increases. In this case, when axial Reynolds is small, critical Taylor number increases according to the following relation:

$$\mathrm{Ta}_{\mathrm{cr}} = \mathrm{Ta}_{\mathrm{cr}}\big|_{\mathrm{Re}_z=0} + 26.5\,\mathrm{Re}_z^2 \tag{3}$$

where

$$\mathrm{Re}_z = U\frac{D_{\mathrm{o}} - D_{\mathrm{i}}}{\upsilon}$$

Combination of axial and rotational flows in the annular air gap resulting from rotation of inner cylinder has been also studied by Kaye *et al.* [4] experimentally. Their observations show that there are four flow regions in the air gap for $\mathrm{Re}_z < 2000$, (a) – laminar flow, (b) – laminar flow with Taylor vortices, (c) – Turbulent flow, and (d) – Turbulent flow with Taylor.

Gu *et al.* [5] observations have shown that in the low velocity axial flows, Taylor kernels are generated roundly. Increasing axial velocity destroys vortexes kernel progressively as vortices kernel has been observed in the very high axial velocity unclearly.

Gazley [6] performed his experiment on the heat transfer in annular flow with 0.43 mm and 8.1 mm air gaps and 63.5 mm radius of rotor in both case of grooved and no grooved rotor. Range of the rotor rotational velocity and axial velocity of air are $0 < w < 4700$ rpm and $0 < U < 90$ m/s, respectively. Results of these experiments the relation of Nusselt number with effective Reynolds number as following:

$$\mathrm{Nu} \approx \mathrm{Re}_{\mathrm{eff}}^{0.8} \tag{4}$$

Where characteristic velocity in Reynolds number is defined as $V_{\mathrm{eff}} = (U^2 + V^2/4)^{(1/2)}$.

Lee [7] has studied heat transfer and pressure loss between two grooved and no grooved coaxial cylinders with rotating one of cylinder experimentally. In this study rotational and axial velocity of rotor ranges are $10^3 < \mathrm{Re}_\varphi < 2\cdot10^7$ and $50 < \mathrm{Re}_z < 1000$, respectively. The result of this study shows when inner the cylinders are grooved, the increase of Taylor number is most effective on increase of outer cylinder Nusselt number.

Kuzay [8] has studied heat transfer of turbulent flow in annulus channel between two coaxial cylinders with rotating inner cylinder experimentally. The surface of inner cylinder is rather insulated and outer cylinder is static and has uniform heat flux. Axial Reynolds and ratio of rotational velocity to axial velocity ranges are $15000 < \mathrm{Re}_z < 65000$ and $0 < V/U < 2.8$, respectively. Results of this research show rotation of inner cylinder increases and decreases temperature of inner and outer cylinder surface respectively, so profile of temperature in radial di-

rection is uniform sensibly. Therefore Nusselt number of combination flow increases when rotational velocity of inner cylinder increases.

Effect of rotation each of the cylinders in annular flow between two coaxial cylinders on distribution of velocity, temperature and heat transfer coefficient of outer cylinder surface has been reported by Beer [9]. In this report fully developed turbulent flow theorem has investigated using Prandtl corrected mixing length model. The diameter of outer cylinder, ratio of inner diameter to outer diameter and ratio of length to air gap hydraulic diameter are 180 mm, $D_i/D_o =$ $= 08575$ and $L/D = 60.94$, respectively. The inner cylinder is insulated and outer cylinder stem from uniform heat flux. Axial Reynolds number and ratio of rotational velocity each of the cylinders to axial velocity ranges are $3000 < \mathrm{Re}_z < 30000$ and $0 < V/U < 4$, respectively. Result of this study shows that rotation of inner cylinder affects more than rotation of outer cylinder on Nusselt number of outer cylinder surface.

Smyth *et al.* [10] have analyzed axial flow forced convective heat transfer on a rotating cylinder numerically. This analysis has been performed two dimensionally and Axisymmetrically. The results show Nusselt number depends on power of 0.8 of Reynolds number.

Kendous [11] has presented an approximate solution for calculating the rate of heat transfer from laminar boundary layer. In this research approximate values quantity of mean Nusselt number by using of an appropriate velocity in the energy equation using the following relation has been obtained.

$$\mathrm{Nu} = 0.6366\sqrt{\mathrm{Re}\,\mathrm{Pr}} \tag{5}$$

Boutarfa *et al.* [12] experimentally have studied flow construction and local heat transfer coefficient of air stream in the air gap between rotor and stator. Temperature of rotor surface is measured by thermography of infra-red ray and analysis flow construction between rotor and stator has performed by particle image velocimetry method. In this study, numerical solution of steady flow energy equation has been done for determining local heat transfer coefficient as well. In this research rotational Reynolds number and ratio of air gap width to rotor radius ranges are $58700 < \mathrm{Re}_\varphi < 176000$ and $0.005 < D_h/D_i < 0.085$, respectively.

Ozerdem [13] investigated forced convective heat transfer from a cylinder in the static air experimentally. In this research, mean heat transfer coefficient has been measured by radiation pyrometer. According to these results $\mathrm{Nu} = 0.318\,(\mathrm{Re}_\varphi)^{0.571}$ which is valid for rotational Reynolds number ranges $2000 < \mathrm{Re}_\varphi < 4000$. These results are in agreement with previous work.

Djaoui *et al.* [14] has studied turbulent heat transfer of air flow between rotor and stator with inner radius grooves experimentally.

Description of experimental apparatus

In fig. 1 schematic of experimental apparatus including motor and generator with apparatus for rotor

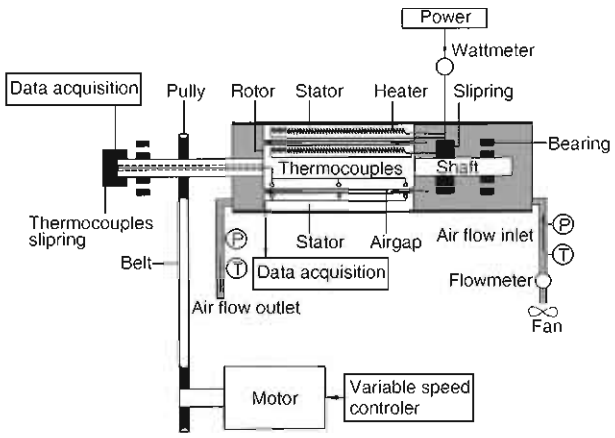

Figure 1. Schematic of experiment apparatus with motor and peripheral rig

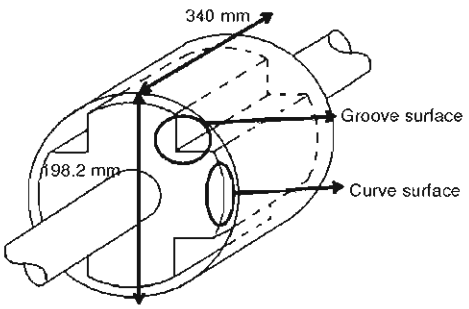

Figure 2. Air gap between rotor and stator with peripheral grooves

revolution adjustment, two pulleys for conveying power between motor and generator rotor, data acquisition system, fan for creation of air flow between rotor and stator, flow meter for mass flow measurement and 28 thermocouples for air temperature measurement, rotor and stator has been shown. In fig. 2, schematic of a generator including two coaxial cylinders as rotor and stator has been shown. Each of them has longitudinal groove in which coils for magnetic field generation have been embedded. The rotor consists of an inner cylinder of aluminum material, with length of 340 mm, diameter of 198.2 mm and inclusion of 4 symmetrical triangular grooves with depth of 26 mm (fig. 2). Stator composed of an outer cylinder of aluminum material, with length of rotor, inner diameter of 214 mm and outer diameter of 300 mm. The air gap between two cylinders, ratio of two diameters and ratio of length to the thickness of air gap are 8 mm, $D_r/D_s = 0.92$ and $L/b = 42.5$, respectively. For simulation of generator performance, thermal elements through holes which have been designed symmetrically and longitudinally with heated electrically have been used. Electrical current transformation to thermal elements is done by slip ring. Generative heat in rotor and stator is adjusted by voltage adjustment apparatus with capacities of 2 and 6 kW, respectively. For preventing heat loss, two ends of cylinders and outer surface of stator are insulated by glass wool. Measurement of temperature axial distribution and heat flux of cylinders surface has been done by thermocouple of type K and with precision of ±1 °C have been installed which at 3 longitudinal positions and two angular positions of cylinder. For preventing air contact with superficial thermocouples, the outer surface of thermocouple is covered by epoxi gum. Generative voltages in thermocouples of inner cylinder connect to monitoring apparatus by means of a temperature slipring. The air flow in air gap between two cylinders is supported by centrifugal fan which is before the channel. Air mass is controlled by a dimer that changes fan revolution. Temperature of inlet and outlet air and air mean velocity at outlet section in 25 locations are measured by thermocouple and pitot tube respectively. The passing air pressure drop is measured by differential pressure gauge that connects to both ends of the channel. The inner cylinder connects variable revolution speed electrical motor by means of conveyor and pulley and variation of its revolution is adjusted by control apparatus. Motor revolution range is $50 < \omega < 1500$ rpm.The Reynolds number range of air axial flow between two cylinders based on hydraulic diameter of air gap is $4000 < Re_z < 30000$.

Uncertainty

Measurement instruments used in this experiment consist of digital Pitot tube with accuracy of 0.1 m/s, 28 thermocouples, wattmeter for measurement of thermal elements Power and rotor and stator electrical power. Uncertainly of thermocouples, temperature indicator, and Pitot tube are ±1 °C, ± 0.1 °C and 1%, respectively. Inaccuracy related to the calculation of heat transfer coefficient always stems from measured parameters such as temperature, velocity and heat flux.

Experiments has been performed at three revolution speeds of 300, 900, 1500 rpm and eight axial Reynolds numbers of 4000, 6000, 9500, 14500, 18000, 22000, 25000, and 30000.

Generative heat by means of thermal elements in rotor and stator is 400 and 1200 W, respectively. By measuring mean velocity at exit section, mass flow and Reynolds number are obtained as:

$$\dot{m} = \rho A U \tag{6}$$

$$\mathrm{Re}_z = \frac{\dot{m} D_\mathrm{h}}{\rho_\mathrm{a} A_\mathrm{gap} \upsilon_\mathrm{a}} \tag{7}$$

Rate of rotor and stator surface heat flux are obtained using temperature gradient at each of surfaces as follows:

$$q_j'' = -k \frac{\partial T_j}{\partial r}\bigg|_\mathrm{R} \cong k \frac{\Delta T_j}{\Delta r}\bigg|_\mathrm{R}, \quad j = r, s \tag{8}$$

where $j = r, s$ are indicator of rotor and stator, respectively, and R is the indicator of surface radius.

For calculating the accuracy of air flow mass in air gap, air mass flow again is calculated by calculation of surfaces total heat transfer rate and measurement of inlet and outlet air temperature:

$$\dot{m} = \frac{\int q'' \mathrm{d}A}{\mathrm{C_p}(T_\mathrm{ao} - T_\mathrm{ai})} \tag{9}$$

where $A = A_\mathrm{r} = A_\mathrm{s}$ and A_r and A_s are area of rotor and stator surface, respectively.

The difference between two mass flows given by relation (6) and (9) is almost 5 percent.

By calculating the rate of rotor and stator surface heat transfer between inlet and each section of length of generator, air mean temperature is obtained as:

$$T_\mathrm{a} = T_\mathrm{ai} + \frac{\int_0^z q'' \mathrm{d}A}{\dot{m} C_p} \tag{10}$$

Relation (11) is derived by substituting from relation (9) into relation (10):

$$T_\mathrm{a} = T_\mathrm{ai} = (T_\mathrm{ao} - T_\mathrm{ai}) \frac{\int_0^z q'' \mathrm{d}A}{\int_0^\mathrm{L} q'' \mathrm{dA}} \tag{11}$$

Finally local and mean heat transfer coefficients of rotor surface are given by:

$$h_r = \frac{q_\mathrm{r}''}{T_\mathrm{r} - T_\mathrm{a}} \tag{12}$$

$$\bar{h}_\mathrm{r} = \frac{1}{L} \int_0^\mathrm{L} h_\mathrm{r} \mathrm{d}z \tag{13}$$

For determining inaccuracy of rotor surface heat transfer coefficient, first by substituting relation (11) into relation (12) and result of it into relation (13):

$$\bar{h}_\mathrm{r} = \frac{1}{L} \int_0^\mathrm{L} \frac{q'' \mathrm{d}z}{T_\mathrm{r} - T_\mathrm{ai} - (T_\mathrm{ao} - T_\mathrm{ai}) \dfrac{\int_0^z q'' \mathrm{d}A}{\int_0^\mathrm{L} q'' \mathrm{d}A}} \tag{14}$$

Relation (14) is simplified to relation (15) by assumption of unvarying rotor and stator heat transfer rate:

$$\bar{h}_r = q''_r \int_0^L \frac{d\left(\frac{z}{L}\right)}{T_r T_{ai} - (T_{ao} - T_{ai})\frac{z}{L}} \tag{15}$$

Method of uncertainty estimation is calculated by Kline [15] due to characteristics of initial measurement inaccuracy as:

$$\left(\frac{\Delta \bar{h}_r}{\bar{h}_r}\right)^2 = \left(\frac{\Delta q''_r}{q''_r}\right)^2 + \left[\frac{\partial \ln I}{\partial (T_r - T_{ai})} d(T_r - T_{ai})\right]^2 + \left[\frac{\partial \ln I}{\partial (T_{ao} - T_{ai})} d(T_{ao} - T_{ai})\right]^2 \tag{16}$$

where

$$I = \int_0^L \frac{d\left(\frac{z}{L}\right)}{T_r - T_{ai} - (T_{ao} - T_{ai})\frac{z}{L}}$$

In these experiments, calculated uncertainty of $\bar{h}$ is nearly 18%.

Results and discussion

The axial Nusselt number of rotor surface at four Reynolds and revolution of 900 rpm has been shown in fig. 3. As shown in fig. 3, Nusselt number of rotor surface at axis direction has declined logarithmically and approaches uniform state at the end. The reason that boundary layer thickness is small at the beginning of air gap and increases at axis direction until it meets to boundary layer of stator surface and flow becomes fully developed. Because of inverse relation of Nusselt number with boundary layer thickness, at the beginning of air gap that boundary layer thickness be minimum, Nusselt number would be maximum and concurrent with fully developing of flow at the end of air gap, Nusselt number approaches to uniform state. Also, as shown in the figure, Nusselt number approaches to uniform state earlier at lower Reynolds. In other words, flow approaches fully developed region earlier. The reason is the decrement of Reynolds causes axial momentum to decrease compared to radial momentum, so boundary layer grows earlier at width of air gap and flow approaches the fully developed region earlier.

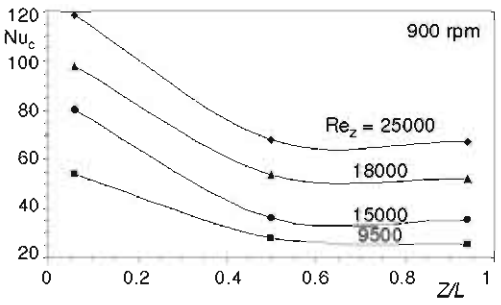

Figure 3. Variations of axial Nusselt number over curve part of rotor at different Reynolds number and revolution of 900 rpm

In fig. 4, the axial Nusselt number distribution of rotor surface has been shown at three revolutions and Reynolds of 18000. As shown in fig. 4, the Nusselt number at revolutions of 300 rpm and 900 rpm in axis direction first decreases and at end approaches to uniform state which indicates flow is fully developed at end of air gap. At rotational speed of 1500 rpm, pressure decreases near the rotor surface at the end of it. This effect causes outside cold air to flow within

the rotor-stator gap and reverse flow is generated as a consequence. This cold flow within the gap increases the heat transfer ratio and Nusselt Number.

Molki *et al.* [16] also observed this phenomenon in his experiments.

In fig. 5, axial Nusselt number distribution of stator surface has been shown at three revolutions and Reynolds of 18000. As shown in fig. 5, by revolution increment, Nusselt number approaches uniform state at the end earlier. The reason is that by revolution increment, centrifugal force of flow increases versus axial momentum and boundary layer thickness increases faster at radial direction and flow approaches to fully developed region earlier. Comparison of this with fig. 4 show that axial distribution of Nusselt number of stator surface is more uniform.

Relation of Nusselt number with Reynolds number in annulus flow between two coaxial cylinders is:

$$\mathrm{Nu} \approx \mathrm{Re}^{0.8} \tag{17}$$

Gazley presented relation of Nusselt number in flow between two coaxial cylinders with rotating inner cylinder as:

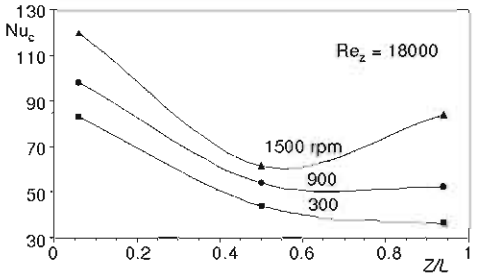

Figure 4. Variations of axial Nusselt number over curve part of rotor at different revolutions and Reynolds number of 18000

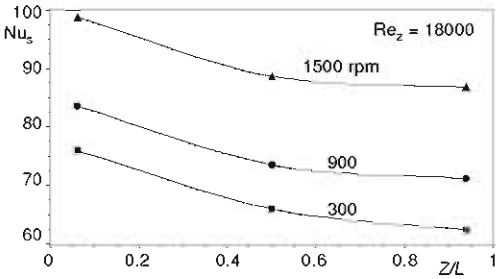

Figure 5. Axial Nusselt number variations of stator surface at different revolutions and Reynolds number of 18000

$$\mathrm{Nu} = 0.022(\mathrm{Re}_{\mathrm{eff}})^{0.8}\,\mathrm{Pr}^{0.5} \tag{18}$$

In this relation, effective Reynolds number is obtained based on effective velocity:

$$V_{\mathrm{eff}} = V_{\mathrm{Z}}\sqrt{1+\left(\frac{V_{\varphi}}{2V_{\mathrm{Z}}}\right)^2} \tag{19}$$

and relation (19) is derived:

$$V_{\mathrm{eff}} = \sqrt{V_z^2+\left(\frac{V_{\varphi}}{2}\right)^2} = V_{\mathrm{Z}}\sqrt{1+\left(\frac{1}{4}\right)\left(\frac{V_{\varphi}}{V_{\mathrm{Z}}}\right)^2} = V_{\mathrm{Z}}\sqrt{1+\left(\frac{V_{\varphi}}{2V_{\mathrm{Z}}}\right)^2}$$

Actually, effective velocity is relative velocity of fluid into surface. By assumption of linear air tangential velocity distribution in width of air gap, mean tangential velocity of air is half tangential velocity of rotor. In fig. 6, mean Nusselt number distribution of stator surface versus effective Reynolds has presented and compared with Gazley,s results. As seen in figure, Nusselt number of stator surface at different revolutions nearly lies on one curve. The comparison between results of present research with results of Gazley indicates Nusselt number in present research is more, because in this research surface of rotor is with groove.

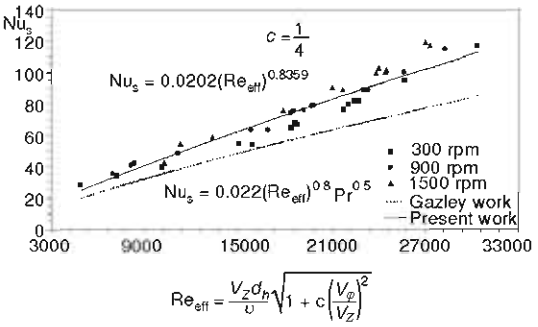

Figure 6. Comparison of stator surface mean Nusselt number distribution *vs.* effective Reynolds number and Gazley's results

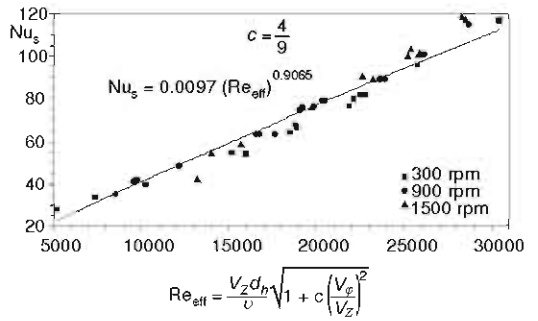

Figure 7. Mean Nusselt number distribution of stator surface versus effective Reynolds number based on 2/3 of tangential velocity of rotor

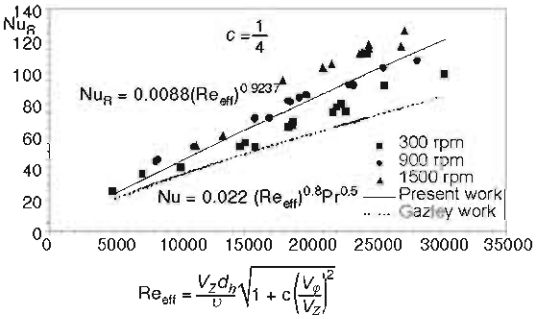

Figure 8. Comparison of rotor total surface means Nusselt number distribution *vs.* effective Reynolds and Gazley results

In fig. 7 Nusselt number distribution of stator surface versus effective Reynolds has been presented but effective velocity has been defined 2/3 based on tangential velocity of rotor. As cleared in this figure, experimental data coincide on a curve better than fig. 6. So it can be said, fluid relative velocity with respect to surface is most important agent in increment of Nusselt number of stator and corresponds with vector addition of axial velocity and 2/3 of rotor tangential velocity.

In fig. 8, mean Nusselt number distribution of rotor surface based on effective Reynolds has been compared with Gazley results. As seen in this figure, experimental data related to different revolutions does not coincide on a curve. For that reason in fig. 9 effective velocities according to vector addition of axial velocity and tangential velocity of rotor has been defined which with this definition proper agreement has been obtained. This shows that fluid relative velocity surface of rotor is more than stator and consequently revolution increment of rotor increases surface heat transfer coefficient of rotor more than stator.

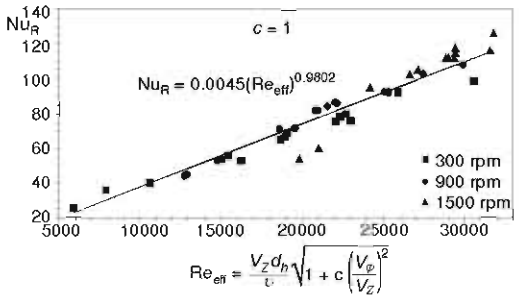

Figure 9. Mean Nusselt number of rotor total surface *vs.* effective Reynolds number

In fig. 10 mean Nusselt number distribution of rotor curve surface has been presented due to effective Reynolds based on tangential velocity of rotor that experimental data have been coincided on a curve properly.

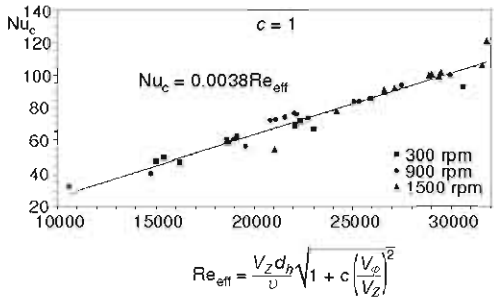

Figure 10. Mean Nusselt number distribution of rotor curve surface *vs.* effective Reynolds number

In fig. 11 mean Nusselt number distribution of rotor grooved surface has been presented effective Reynolds based on 1/2 of rotor tangential velocity. A multiple 1/2 of rotor tangential velocity in effective velocity shows that increment of revolution noticeably result in increment of relative velocity and increment of rotor grooved surface heat transfer coefficient. The reason is that by rotation of rotor, air impacts grooved surface and slides into grooved surface and as a result air relative velocity in addition to components of tangential and axial velocity has radial component as well.

In fig. 12 the air pressure loss variations has been presented due to effective Reynolds as passing from air gap between rotor and stator. The pressure loss in the annulus flow without rotation is given by Reynolds number of power 2 whereas in this figure by Reynolds number of power 2.5. This shows effect of rotor rotation on increment of pressure loss.

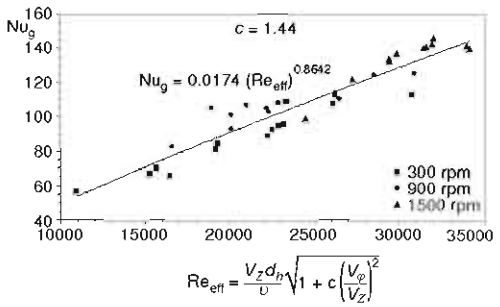

Figure 11. Mean Nusselt number distribution of rotor grooved surface *vs.* effective Reynolds number

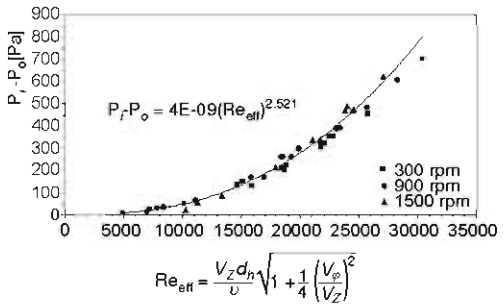

Figure 12. Variations of air pressure loss *vs.* efective Reynolds number

Conclusions

The important results of this research include:

- by increment of rotor revolution from 300 rpm until 1500 rpm, heat transfer coefficient of rotor and stator increases 45 and 30%, respectively, and this rate of increment is more at lower Reynolds number,
- by increment of velocity ratio V_φ/V_m air flow approaches to fully developed state earlier,
- heat transfer coefficient axial distribution of stator surface is more uniform than Heat transfer coefficient axial distribution of rotor surface,
- by increment of velocity ratio V_φ/V_m, probability of inverse flow increases at outlet air gap,
- the effective velocity for stator is defined as $V_{eff} = [V_Z^2 + (2V\varphi/3)^2]^{(1/2)}$ and, $V_\varphi = rw$,
- the effective velocity for rotor curve surface is defined as $V_{eff} = (V_Z^2 + V_\varphi^2)^{(1/2)}$,
- the effective velocity for rotor grooved surface is defined as $V_{eff} = (V_Z^2 + (1.2\ V_\varphi)^2]^{(1/2)}$, and
- the relation of pressure drop due to effective Reynolds number between rotor and stator is $\Delta p \approx (Re_{eff})^{2.521}$.

Nomenclature

A – area, [m^2]
b – radial distance between rotor and stator, [m]
C_p – specific heat at constant pressure, [JK^{-1}]
h – heat transfer coefficient, [$Wm^{-2}K^{-1}$]
D – diameter, [m]
d_h – hydraulic diameter, [m]
k – thermal conductivity coefficient, [$Wm^{-1}k^{-1}$]
L – length, [m]
$\dot{m}$ – mass flow, [kgs^{-1}]
Nu_l – Nusselt number (= hl/k), [–]
p – pressure, [Pa]
$\dot{Q}$ – total heat rate, [W]
q'' – heat transfer rate, [Wm^{-2}]
Re – Reynolds number (= UD/υ), [–]
r – radial direction, [–]
T – temperature, [K]
Ta – Teylor number,
– (=$[V(D_o - D_i)2\upsilon](D_h/D_m)^{1/2}$, [–]
U – mean axial velocity, [ms^{-1}]
V – tangential velocity, [ms^{-1}]
z – axial direction, [–]
u – velocity, [ms^{-1}]

Greek symbols

Δ – difference
θ – non-dimensional temperature, [–]
υ – kinematic viscosity, [m^2s^{-1}]
ρ – density, [kgs^{-1}]
φ – tangential direction, [–]
ω – rotational velocity, [s^{-1}]

Subscripts

a – air
cr – critical
eff – effective
h – hydraulic
i – inner
o – outer
r – rotor
s – stator
z – axial

Superscript

$\bar{}$ – mean

Reference

[1] Taylor, G. I., Stability of a Viscous Liquid Contained between Two Rotating Cylinders, Phil. Trans R. Soc. Lond. A223, 1923, pp. 289-343
[2] Pia, S. I., Turbulent Flow between Rotating Cylinders, NACATN 892, 1943
[3] Chandrasekhar, S., The Stability of Spiral Flow between Rotating Cylinders, *Proceedings*, R. Soc. Lond, A265, 1961, pp. 188-196
[4] Kaye, J., Elgar, E. C., Modes of Adiabatic and Diabatic Fluid Flow in an Annulus with an Inner Rotating Cylinder, *J. Heat Transfer, 80* (1958), 5, pp. 753-765
[5] Gu, Z. H., Fahidy, T. Z., Visualization of Flow Patterns in Axial Flow between Horizontal Coaxial Rotating Cylinder, *Can. J. Chem. Engng., 63* (1985), 1, pp. 14-21
[6] Gazley, G., Heat Transfer Characteristic of Rotational and Axial between Concentric Cylinders, *Trans. ASME, 80* (1958), 5, pp. 79-90
[7] Lee, Y. N., Heat Transfer Characteristics of the Annulus of Two Coaxial Cylinders One Cylinder Rotating, *Int. J. Heat Mass Transfer, 32* (1989), 4, pp. 711-722
[8] Kuzay, T. M., Turbulent Heat and Momentum Transfer Studies", Ph. D. thesis, University of Minnesota, Minneapolis, Minn., USA, 1973
[9] Pfitzer, H., Beer, H., Heat Transfer in an Annulus between Independently Rotating Tubes with Turbulent Axial Flow, *Int. J. Heat Mass Transfer, 35* (1992), 3, pp. 623-633
[10] Smyth, R., Zurita, P., Heat Transfer at the outer Surface of a Rotating Cylinder in the Presence of Axial Flow, *Transaction on Engineering Sciences, 5*, 1994, WIT Press, Southampton, UK, www-witness.com
[11] Kendoush, A. A., An Approximate Solution of the Convective Heat Transfer from an Isothermal Rotating Cylinder, *International Journal of Heat and Fluid Flow, 17* (1996), 4, pp. 439-441
[12] Boutarfa, R., Harmand, S., Local Convective Heat Exchanges and Flow Structure in a Rotor- Stator System, *International Journal of Thermal Science, 42* (2003), 12, pp. 1129-1143
[13] Ozerdem, B., Measurements of Convective Heat Transfer Coefficient for a Horizontal Cylinder Rotating in Quiescent Air, *International Communications in Heat and Mass Transfer, 27* (2000), 3, pp. 389-395
[14] Djaoui, M., Debuchy, R., Heat Transfer in a Rotor-Stator System with a Radial Inflow, *Mechanics Physics Chemistry Astronomy, 32* (1998), 5, pp. 309-314

[15] Kline, S. J., Mclintock, M. T., Describing Uncertainties in Single-Sample Experiments, *Mech. Eng.*, *75* (1953), 1, pp. 3-8
[16] Molki, M., Astill, K. N., Convective Heat-Mass Transfer in the Entrance Region of a Concentric Annulus Having a Rotating Inner Cylinder, *Int. Journal of Heat and Fluid Flow, 11* (1990), 2, pp. 120-128

Paper submitted: July 2, 2011
Paper revised: December 3, 2011
Paper accepted: December 11, 2011